Time-Domain Analysis for the Coupling Problem of Overhead Lines above Multilayered Earth

Ayoub Lahmidi and Abderrahman Maaouni*

Abstract—This paper investigates the effect of an external plane wave on a multi-conductor transmission line (MTL) located above a multilayer soil directly in the time domain. An improved finite-difference time-domain (FDTD) method is used, in conjunction with Vector Fitting (VF), to obtain the recursion relations of voltages and currents along the line by discretizing the equations in time and one-dimensional space. The source terms of the coupling equations are efficiently obtained in the time domain based on the Gaver-Stehfest algorithm. An equivalent model is also established in this work, where the geometry with three conductors is reduced to two conductors. Finally, some examples are presented to illustrate the effect of the soil and the plane wave on the transient.

1. INTRODUCTION

Electromagnetic field interaction with transmission lines is an important topic in electromagnetic compatibility [1]. Many researchers have investigated the field-to-transmission line coupling by calculating the transient currents and voltages induced on the line. In most cases, the authors assumed that the multi-wire structure is placed above a homogeneous medium, but a few works have involved the case of stratified medium. Doric et al. in [2] deal with the plane wave coupling to multiple transmission lines over lossy half-space for an arbitrary angle of incidence. The influence of the lossy half-space has been taken into account via the reflection coefficient (RC) approximation instead of the Sommerfeld integral approach. Rachidi in [3] evaluates the time-domain representation of transmission line above a homogeneous medium. The general expression for the ground impedance had been invested in the time domain using the inverse Fourier transform. The authors in [4] developed an efficient method for modeling a dispersive transmission line illuminated by an external field in the presence of a homogeneous ground. The transmission line is represented as a two-port stamp which only included resistive elements and dependent current sources. The time-domain analysis of transmission line coupling to external plane wave requires an expression for the transient reflected field from a finitely conducting half-space. This means that it is appropriate to find a time-domain representation of the Fresnel coefficients (FC). Barnes and Tesche [5] developed an approximate analytical expression for the transient earth-reflected field. The approximation reached from the inversion of the Laplace transform led to good results only for large values of the elevation angle. Other methods based on the decomposition of the frequency-domain (FC) into space-dependent and space-frequency-dependent functions are presented by Antonijevic and Poljak in [6]. The space-frequency-dependent function is derived by using Graver-Stehfest algorithm [7].

The transient analysis of transmission line plane wave coupling above a stratified medium in the time domain has been the subject of a few studies. Lu et al. [8] present a new method in time domain to consider the effect of the multilayer soil based on the complex ground return plane and a continuous variation of the surface impedance between layers, but the displacement current was not considered.

Transient analysis of incident field coupling to multiconductor transmission lines has been the subject treated in [9] by using the complex ground return plane method presented in [8] and the (FC) in the frequency domain.

The aim of the paper is to present an efficient method for the time domain analysis of plane wave coupling to an overhead line in the presence of multilayer earth. The formulation of transmission line equations is based on the Agrawal model [10] involving only the external electric field components in distributed sources along the line. The inclusion of Fresnel coefficients to estimate the distributed sources is straightforward for numerical calculations in the frequency domain but becomes complicated if their time domain counterparts are needed due to the difficulty in finding time analytical expressions of (FC) for stratified medium. In this paper, a novel expression of (FC) is presented by exploiting the method proposed in [6] and the expressions of the reflection coefficients in frequency domain for stratified medium developed in [11].

To attain a correct evaluation of transients on overhead lines above lossy stratified earth, an appropriate choice of the earth-return impedance is needed. In this work, the Nakagawa model is adopted [12], and the choice of this model is based on the fact that it takes into consideration the propagation effect contrary to the Sunde model [13] used by Rachidi in [3]. The vector fitting developed in [14] is used to reach a time-domain expression of this model [12]. To characterize the transmission line in the time domain, we use in this work the FDTD in leap-frog scheme [15, 16], and finally an equivalent model of multiple conductor systems is presented.

2. TRANSMISSION LINE EQUATIONS

Consider N_c uniform conductors with the same radius r, at a position x_i and a height y_i ($i = 1, 2, \ldots, N_c$) parallel to z-axis; the sub-index i denotes the particular wire of the multiconductor line. The wired structure is located above a stratified medium, which is composed of three layers. Each layer is characterized by a constant permittivity $\epsilon_j = \epsilon_0 \epsilon_{rgj}$, permeability $\mu_j = \mu_0$, and conductivity σ_j ($j = 1, 2, 3$). μ_0 and ε_0 are electrical parameters of the free space. The structure is excited by an arbitrary polarization plane wave as shown in Fig. 1.
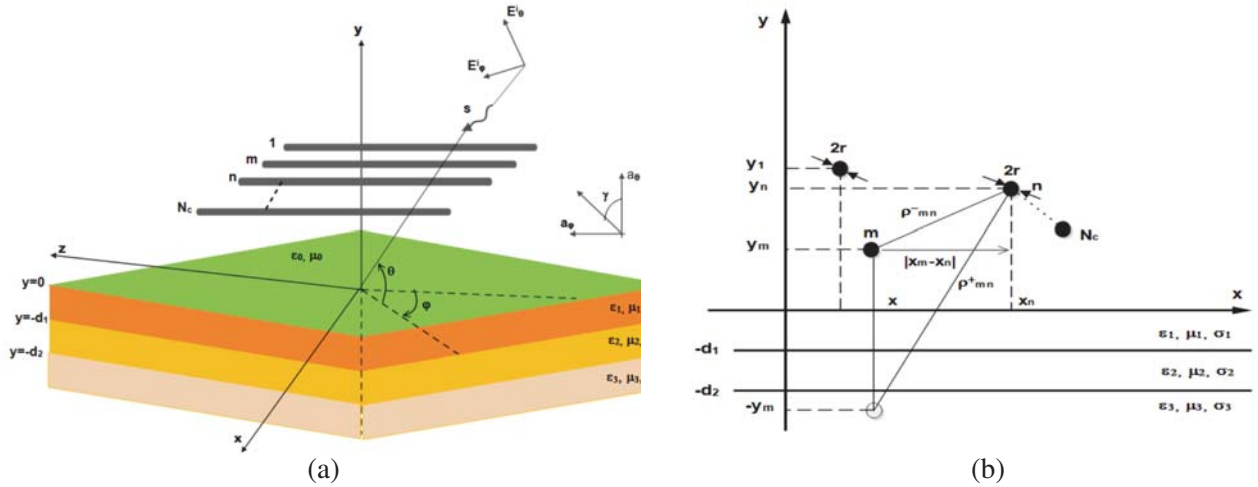

Figure 1. Geometry of multiconductor transmission line above stratified earth excited by a plane wave. (a) Geometric configuration of the line. (b) Cross-section of the wired structure.

The MTL equations for the general case for these conductors immersed in an incident field are expressed for the voltage vector $\mathbf{V}(z, t)$ and current vector $\mathbf{I}(z, t)$ in the time domain at a position z as follows

$$\frac{\partial \mathbf{V}(z,t)}{\partial z} + \mathbf{Z}(t) \circledast \mathbf{I}(z,t) = \mathbf{V}_F^s(z,t) \tag{1}$$

$$\frac{\partial \mathbf{I}(z,t)}{\partial z} + \mathbf{C}\frac{\partial \mathbf{V}(z,t)}{\partial t} = \mathbf{I}_F^s(z,t) \tag{2}$$

$\mathbf{V}_F^s(z,t)$ and $\mathbf{I}_F^s(z,t)$ represent the source terms which can be expressed as

$$\mathbf{V}_F^s(z,t) = \tilde{\mathbf{E}}_z(z,t) - \frac{\partial \mathbf{E}_T(z,t)}{\partial z} \tag{3}$$

$$\mathbf{I}_F^s(z,t) = -\mathbf{C}\frac{\partial \mathbf{E}_T(z,t)}{\partial t} \tag{4}$$

where $\tilde{\mathbf{E}}_z(z,t) = \mathbf{E}_z(x,h,z,t) - \mathbf{E}_z(x,0,z,t)$, $\mathbf{E}_T(z,t) = \int_0^h \mathbf{E}_y dy$, and $\mathbf{E}_z$, $\mathbf{E}_y$ are z and y axis components of the primary electric field, respectively.

The time domain expression of the impedance $\mathbf{Z}(t)$ is obtained by applying the Vector Fitting method [14] on the frequency-dependent series impedance matrix $\mathbf{Z}$,

$$\mathbf{Z}(t) \Leftrightarrow \mathbf{Z} = \mathbf{Z}_w + \mathbf{Z}_e \tag{5}$$

where $\mathbf{Z}_w$ represents the per-unit-length internal impedance of the conductors in the cable system. For thin solid conductors, $\mathbf{Z}_w$ is defined as [17]

$$Z_{w,mn} \simeq \delta_{mn}\left(\frac{k_{wn}}{2\pi r\sigma_{wn}}\right)\frac{I_0(k_{wn}r)}{I_1(k_{wn}r)}, \qquad \delta_{mn} = \begin{cases} 1, & m=n \\ 0, & m\neq n \end{cases} \tag{6}$$

In Eq. (6), $k_{wn} = \sqrt{s\mu_{wn}(\sigma_{wn} + s\varepsilon_{wn})}$ and μ_{wn}, ε_{wn}, σ_{wn}, are the electrical parameters of the nth conductor. I_0 and I_1 are the modified Bessel functions. The influence of the earth return path $\mathbf{Z}_e$ is expressed by

$$\mathbf{Z}_e = s\mathbf{L} + \frac{s\mu_0}{\pi}\mathbf{J} \tag{7}$$

where $\mathbf{L}$ is the per-unit-length inductance matrix whose elements are

$$L_{mn} = \frac{\mu_0}{2\pi}\ln\left(\frac{\rho_{mn}^*}{\rho_{mn}}\right), \tag{8}$$

with $\rho_{mn} = \sqrt{(x_m - x_n)^2 + (y_m - y_n)^2}$ and $\rho_{mn}^* = \sqrt{(x_m - x_n)^2 + (y_m + y_n)^2}$. For a single conductor $\rho_{mn} = r$ and $\rho_{mn}^* = 2y_n$ $(m = n)$.

By adopting the Nakagawa model [12] for the three-layer earth, the matrix of conduction losses in the ground $\mathbf{J}$ is given by

$$[\mathbf{J}]_{mn} = \int_0^\infty \chi^{(s)} e^{-(y_m + y_n)\nu}\cos(|x_m - x_n|\nu)d\nu \tag{9}$$

where

$$\chi^{(s)} = \frac{c_1 + c_2}{(\nu + \mu_0 b_1)c_1 + (\nu - \mu_0 b_1)c_2} \tag{10}$$

$$c_1 = (b_1 + b_2)(b_2 + b_3) + (b_1 - b_2)(b_2 - b_3) \times e^{2a_2(d_1 - d_2)}$$

$$c_2 = ((b_1 - b_2)(b_2 + b_3) + (b_1 + b_2)(b_2 - b_3) \times e^{2a_2(d_1 - d_2)}) \times e^{-2a_1 d_1}$$

$$a_i = \sqrt{v^2 + k_i^2 - k_0^2}, \; b_i = a_i/\mu_i, \quad i = 1, 2 \text{ and } 3$$

In Eq. (10), k_0 and $k_i = \sqrt{s\mu_i(\sigma_i + s\varepsilon_i)}$ $(i = 1, 2 \text{ and } 3)$ are the propagation constants in the air and in the ith layer, respectively.

By following the same process consisting of the introduction of the poles and the residues deduced from the Vector Fitting method in the MTL equations, as indicated in [19], Eq. (1) can be expressed as

$$\frac{\partial \mathbf{V}(z,t)}{\partial z} + (\mathbf{L} + \mathbf{D})\frac{\mathbf{I}(z,t)}{\partial t} + (\mathbf{R} - \mathbf{\Omega})\mathbf{I}(z,t) + \phi(t) \circledast \frac{\partial}{\partial t}\mathbf{I}(z,t) = \mathbf{V}_F^s(z,t) \tag{11}$$

where

$$\mathbf{\Omega} = \sum_{i=1}^M \frac{\kappa_i}{p_i}, \quad \phi = \sum_{i=1}^M \frac{\kappa_i}{p_i}e^{p_i t} \tag{12}$$

$\mathbf{D}$ and $\mathbf{R}$ are a proportional term and a constant term, respectively. κ_i and p_i are complex quantities that represent the residues and poles.

3. ELECTRIC FIELD

In order to study the plane wave coupling to overhead lines over stratified soil, the primary field composed of the incident electric field $\mathbf{e}^i(t)$ and the field $\mathbf{e}^r(t)$ reflected from the soil [18] is needed to obtain explicit expressions of the distributed voltage and current sources along the line.

The general expression of the primary field in the time domain $\mathbf{E}(t)$ above the stratified medium is

$$\mathbf{E}(t) = \mathbf{e}^i(t) + \mathbf{e}^r(t) \tag{13}$$

The time domain expressions of $E_z(t)$ and $E_y(t)$, which appear in Eqs. (3) and (4), are given as

$$E_y(t) = \left(\cos(\gamma)\cos(\theta)e_0(t - t_0^-) + \cos(\gamma)\cos(\theta)\gamma_v \circledast e_0\left(t - t_0^+\right)\right) \tag{14}$$

$$E_z(t) = \left(\cos(\gamma)\sin(\theta)\sin(\phi) + \sin(\gamma)\sin(\phi)\right)e_0(t - t_0^-)$$
$$+ \left(-\gamma_v\cos(\gamma)\sin(\theta)\sin(\phi) + \gamma_h\sin(\gamma)\sin(\phi)\right) \circledast e_0\left(t - t_0^+\right)) \tag{15}$$

with $t_0^\pm = \sqrt{\epsilon_0\mu_0}(-\cos(\theta)\sin(\phi)x \pm \sin(\theta)y + \cos(\theta)\cos(\phi)z)$, and γ_v, γ_h are the Fresnel coefficients in the time domain. $\circledast$ is the convolution product, $\delta(\cdot)$ the impulse function, and $u(\cdot)$ the unit step function. $e_0(t)$ is the two-exponential shape which is often used to simulate high-altitude Electromagnetic pulses (HEMP) and is given by

$$e_0(t) = E_0\left(e^{-\alpha t} - e^{-\beta t}\right)u(t) \tag{16}$$

The parameters in Eq. (16) assume the following values: $\alpha = 4.086 \times 10^6\,\text{s}^{-1}$, $\beta = 1.565 \times 10^8\,\text{s}^{-1}$, $E_0 = V_0/l_0$, $V_0 = 56.6kV$, $l_0 = 1\,\text{m}$.

Evaluating expressions (14) and (15) requires the use of a direct time domain expression of the reflection coefficient function. In this work, the time domain (FC) function is derived by transforming the frequency domain (FC) function for the stratified medium presented in [11] into the time-domain using the Stehfest algorithm [7]. This method approximates the time domain (FC) function as

$$\gamma_\Upsilon(t, \theta) = \gamma_\Upsilon'(\theta)\delta(t) + \frac{\ln 2}{t}\sum_{i=1}^N \widetilde{V}_i \Gamma_\Upsilon''\left(\frac{i\ln 2}{t}, \theta\right) \tag{17}$$

where $\widetilde{V}_i$ is described by the following relationship

$$\widetilde{V}_i = (-1)^{i+\frac{N}{2}} \sum_{k=\left(\frac{i+1}{2}\right)}^{\min\left(i, \frac{N}{2}\right)} \frac{k^{\frac{N}{2}}(2k)!}{\left(\frac{N}{2} - k\right)!k!(k-1)!(2k-i)!} \tag{18}$$

The parameter N is called the Stehfest number. Parameter N must be an even integer, and it should be chosen by trial and error method. Thus, a suitable choice of N is important to achieve the most accurate solution. In this work, the optimal value to accurately obtain the primary field is equal to 10.

In Eq. (17), $\gamma_\Upsilon'(\theta)$ and Γ_Υ'' are defined by

$$\begin{cases} \gamma_\Upsilon'(\theta) = \lim_{s \to \infty} \Gamma_\Upsilon(s, \theta), \\ \Gamma_\Upsilon''(s, \theta) = \Gamma_\Upsilon(s, \theta) - \gamma_\Upsilon'(\theta) \end{cases} \tag{19}$$

with

$$\Gamma_\Upsilon = \frac{\left(\Lambda_{11} + \Lambda_{12}P\Upsilon_{k=M_L}\right)P\Upsilon_{k=1} - \left(\Lambda_{21} + \Lambda_{22}P\Upsilon_{k=M_L}\right)}{\left(\Lambda_{11} + \Lambda_{12}P\Upsilon_{k=M_L}\right)P\Upsilon_{k=1} + \left(\Lambda_{21} + \Lambda_{22}P\Upsilon_{k=M_L}\right)},$$

$$P\Upsilon_k = \begin{cases} \Upsilon = v, P\Upsilon_k = \dfrac{\sqrt{\dfrac{\mu_0}{\epsilon_0}}\sqrt{n_k^2 - \cos^2(\theta)}}{\epsilon_{rg_k}\left(1 + \dfrac{\sigma_k}{s\epsilon_k}\right)}, \\ \\ \Upsilon = h, P\Upsilon_k = \sqrt{n_k^2 - \cos^2(\theta)}\sqrt{\dfrac{\epsilon_0}{\mu_0}} \end{cases} \tag{20}$$

Λ_{nl} are the elements of the characteristic matrix Λ of the stratified medium. Λ is expressed as follows

$$\Lambda = \prod_{k=1}^{M_L-1} \Lambda_k = \prod_{k=1}^{M_L-1} \begin{bmatrix} \cosh(q_k) & \dfrac{1}{P_{\Upsilon_k}} \sinh(q_k) \\ P_{\Upsilon_k} \sinh(q_k) & \cosh(q_k) \end{bmatrix}, \tag{21}$$

$$q_k = s(d_k - d_{k-1})\sqrt{\epsilon_0 \mu_0}\sqrt{n_k^2 - \cos^2(\theta)}, \ d_{-1} = 0$$

where $n_k = \sqrt{\mu_{r_k}\epsilon_{r_k} + \frac{\mu_{r_k}\sigma_k}{(\epsilon_0 s)}}$ is the complex refractive index of the k-th layer, M_L the number of soil layers, and s the complex frequency.

Given the nature of the waveform, i.e., a biexponential, the convolution product $\gamma_\Upsilon \circledast e_0(t)$ appearing in expressions (14) and (15) is accurately calculated using the recursive convolution introduced in [18].

4. DISCRETIZATION OF THE MTL EQUATIONS

The MTL equations are discretized both in time and space by using the FDTD method in a leap-frog manner [19]. The transmission line is divided into K segments, each of length Δz. Each voltage and adjacent current solution point are separated by $\frac{\Delta z}{2}$. In addition, the time points are also interlaced, and each voltage time point and adjacent current time point are separated by $\frac{\Delta t}{2}$. The two ends of the line are separated by a length l_z and connected to a resistive circuit. Discretizing the derivatives in the transmission-line Eqs. (2) and (11) using second-order central differences gives

$$\frac{\mathbf{V}_{k+1}^n - \mathbf{V}_k^n}{\Delta z} + (\mathbf{L} + \mathbf{D})\frac{\mathbf{I}_{k+\frac{1}{2}}^{n+\frac{1}{2}} - \mathbf{I}_{k+\frac{1}{2}}^{n-\frac{1}{2}}}{\Delta t} + \int_0^{n\Delta t} \phi(\tau)\frac{\partial}{\partial(n\Delta t - \tau)}\mathbf{I}_{k+\frac{1}{2}}(n\Delta t - \tau)\, d\tau$$

$$+(\mathbf{R} - \mathbf{\Omega})\frac{\mathbf{I}_{k+\frac{1}{2}}^{n+\frac{1}{2}} + \mathbf{I}_{k+\frac{1}{2}}^{n-\frac{1}{2}}}{2} = \frac{\tilde{\mathbf{E}}_{z,k+\frac{1}{2}}^{n+\frac{1}{2}} + \tilde{\mathbf{E}}_{z,k+\frac{1}{2}}^{n-\frac{1}{2}}}{2} - \frac{\mathbf{E}_{T,k+1}^n - \mathbf{E}_{T,k}^n}{\Delta z}$$

$$\frac{\mathbf{I}_{k+\frac{1}{2}}^{n+\frac{1}{2}} - \mathbf{I}_{k-\frac{1}{2}}^{n+\frac{1}{2}}}{\Delta z} + \mathbf{C}\frac{\mathbf{V}_k^{n+1} - \mathbf{V}_k^n}{\Delta t} = \mathbf{G}_1\left(\mathbf{E}_{T,k}^{n+1} - \mathbf{E}_{T,k}^n\right) \tag{22}$$

where $\mathbf{G}_1 = -\frac{1}{\Delta t}\mathbf{C}$, and k and n are space and time indices, respectively.

In this work, the time derivative of the current which appears in the convolution integral in Eq. (22) can be approximated using the piecewise polynomial approximation [19] as follows

$$\frac{\partial}{\partial t}\mathbf{I}_{k+\frac{1}{2}}(t - \tau) \tag{23}$$

$$= \frac{\partial}{\partial t}\mathbf{I}_{k+\frac{1}{2}}(t - m\Delta t) - \frac{\frac{\partial}{\partial t}\mathbf{I}_{k+\frac{1}{2}}(t - (m+1)\Delta t) - \frac{\partial}{\partial t}\mathbf{I}_{k+\frac{1}{2}}(t - (m-1)\Delta t)}{2\Delta t}(\tau - m\Delta t)$$

$$+ \frac{\frac{\partial}{\partial t}\mathbf{I}_{k+\frac{1}{2}}(t - (m+1)\Delta t) - 2\frac{\partial}{\partial t}\mathbf{I}_{k+\frac{1}{2}}(t - m\Delta t) + \frac{\partial}{\partial t}\mathbf{I}_{k+\frac{1}{2}}(t - (m-1)\Delta t)}{2\Delta t^2}(\tau - m\Delta t)^2 \tag{24}$$

By using the central difference scheme at $n\Delta t$ to approximate the time derivatives of $\mathbf{I}_{k+\frac{1}{2}}$, we get after some manipulations

$$\phi(t) \circledast \frac{\partial}{\partial t}\mathbf{I}_{k+\frac{1}{2}}(t)\bigg|_{t=n\Delta t} = \sum_{i=1}^M \frac{\kappa_i}{p_i} \sum_{\substack{1\leq m\leq n, \\ m, \text{ odd}}} (\mathbf{A}_m\chi_i^m + \mathbf{B}_m\xi_i^m + \mathbf{C}_m\eta_i^m) \tag{25}$$

where

$$\mathbf{A}_m = \mathbf{I}_{k+\frac{1}{2}}^{n-m+\frac{1}{2}} - \mathbf{I}_{k+\frac{1}{2}}^{n-m-\frac{1}{2}}$$

$$\mathbf{B}_m = \mathbf{I}_{k+\frac{1}{2}}^{n-m-\frac{1}{2}} - \mathbf{I}_{k+\frac{1}{2}}^{n-m-\frac{3}{2}} - \mathbf{I}_{k+\frac{1}{2}}^{n-m+\frac{3}{2}} + \mathbf{I}_{k+\frac{1}{2}}^{n-m+\frac{1}{2}}$$

$$\mathbf{C}_m = 3\mathbf{I}_{k+\frac{1}{2}}^{n-m-\frac{1}{2}} - \mathbf{I}_{k+\frac{1}{2}}^{n-m-\frac{3}{2}} + \mathbf{I}_{k+\frac{1}{2}}^{n-m+\frac{3}{2}} - 3\mathbf{I}_{k+\frac{1}{2}}^{n-m+\frac{1}{2}}$$

The quantities χ_i^m, ξ_i^m, and η_i^m are given by

$$\chi_i^m = \frac{2e^{p_i m \Delta t} \sinh p_i \Delta t}{p_i \Delta t}$$

$$\xi_i^m = -\frac{e^{p_i m \Delta t}(p_i \Delta t \cosh(p_i \Delta t) - \sinh(p_i \Delta t))}{(p_i \Delta t)^2}$$

$$\eta_i^m = \frac{e^{p_i m \Delta t}(-2p_i \Delta t \cosh(p_i \Delta t) + (2 + (p_i \Delta t)^2) \sinh(p_i \Delta t))}{(p_i \Delta t)^3}$$

By inserting these terms in Eq. (25), we obtain the following relationship

$$\phi(t) \circledast \frac{\partial}{\partial t} \mathbf{I}_{k+\frac{1}{2}}(t)\bigg|_{t=n\Delta t} = \sum_{i=1}^{M} \frac{\kappa_i}{p_i} \left[\left(\mathbf{A}_1 \chi_i^1 + \mathbf{B}_1 \xi_i^1 + \mathbf{C}_1 \eta_i^1\right) + \mathbf{\Psi}_i^n \right]$$

with

$$\mathbf{\Psi}_i^n = \left(\left(\mathbf{I}_{k+\frac{1}{2}}^{n-\frac{5}{2}} - \mathbf{I}_{k+\frac{1}{2}}^{n-\frac{7}{2}} \right) \chi_i^3 + \left(\mathbf{I}_{k+\frac{1}{2}}^{n-\frac{7}{2}} - \mathbf{I}_{k+\frac{1}{2}}^{n-\frac{9}{2}} - \mathbf{I}_{k+\frac{1}{2}}^{n-\frac{3}{2}} + \mathbf{I}_{k+\frac{1}{2}}^{n-\frac{5}{2}} \right) \xi_i^3 \right.$$
$$\left. + \left(3\mathbf{I}_{k+\frac{1}{2}}^{n-\frac{7}{2}} - \mathbf{I}_{k+\frac{1}{2}}^{n-\frac{9}{2}} + \mathbf{I}_{k+\frac{1}{2}}^{n-\frac{3}{2}} - 3\mathbf{I}_{k+\frac{1}{2}}^{n-\frac{5}{2}} \right) \eta_i^3 \right) + e^{2p_i \Delta t} \mathbf{\Psi}_i^{n-2}, \tag{26}$$

and

$$\mathbf{A}_1 = \mathbf{I}_{k+\frac{1}{2}}^{n-\frac{1}{2}} - \mathbf{I}_{k+\frac{1}{2}}^{n-\frac{3}{2}} \tag{27}$$

$$\mathbf{B}_1 = \mathbf{I}_{k+\frac{1}{2}}^{n-\frac{3}{2}} - \mathbf{I}_{k+\frac{1}{2}}^{n-\frac{5}{2}} - \mathbf{I}_{k+\frac{1}{2}}^{n+\frac{1}{2}} + \mathbf{I}_{k+\frac{1}{2}}^{n-\frac{1}{2}} \tag{28}$$

$$\mathbf{C}_1 = 3\mathbf{I}_{k+\frac{1}{2}}^{n-\frac{3}{2}} - \mathbf{I}_{k+\frac{1}{2}}^{n-\frac{5}{2}} + \mathbf{I}_{k+\frac{1}{2}}^{n+\frac{1}{2}} - 3\mathbf{I}_{k+\frac{1}{2}}^{n-\frac{1}{2}} \tag{29}$$

In order to obtain the transient current and voltage on an overhead line above a stratified medium, Eq. (22) should be solved for $\mathbf{V}_k^{n+1}$, and Eq. (22) for $\mathbf{I}_{k+\frac{1}{2}}^{n+\frac{1}{2}}$. Referring to the previous relations, it is obvious to show that the general solution of the transmission line equations for $\mathbf{V}_k^{n+1}$ and $\mathbf{I}_{k+\frac{1}{2}}^{n+\frac{1}{2}}$ can be written as

$$\mathbf{I}_{k+\frac{1}{2}}^{n+\frac{1}{2}} = \mathbf{Z}_1^{-1} \left(\mathbf{Z}_2 \mathbf{I}_{k+\frac{1}{2}}^{n-\frac{1}{2}} - \left(\mathbf{V}_{k+1}^n - \mathbf{V}_k^{n+1} \right) + \mathbf{Z}_3 \mathbf{I}_{k+\frac{1}{2}}^{n-\frac{3}{2}} + \mathbf{Z}_4 \mathbf{I}_{k+\frac{1}{2}}^{n-\frac{5}{2}} \right.$$
$$\left. -\Delta z \left(\mathbf{\Psi}^n - \left(\frac{\tilde{\mathbf{E}}_{z,k+\frac{1}{2}}^{n+\frac{1}{2}} + \tilde{\mathbf{E}}_{z,k+\frac{1}{2}}^{n-\frac{1}{2}}}{2} - \frac{\mathbf{E}_{T,k+1}^n - \mathbf{E}_{T,k}^n}{\Delta z} \right) \right) \right) \tag{30}$$

$$\mathbf{V}_k^{n+1} = \mathbf{V}_k^n - \frac{1}{\varepsilon_0 \mu_0} \left(\frac{\Delta t}{\Delta z} \right) \mathbf{L} \left(\left(\mathbf{I}_{k+\frac{1}{2}}^{n+\frac{1}{2}} - \mathbf{I}_{k-\frac{1}{2}}^{n+\frac{1}{2}} \right) - \Delta z \left(\mathbf{G}_1 \left(\mathbf{E}_{T,k}^{n+1} - \mathbf{E}_{T,k}^n \right) \right) \right) \tag{31}$$

where

$$\mathbf{Z}_1 = \Delta z \left(\frac{(\mathbf{L} + \mathbf{D})}{\Delta t} + \frac{\mathbf{R}}{2} - \frac{\mathbf{\Omega}}{2} - \xi + \eta \right)$$

$$\mathbf{Z}_2 = \Delta z \left(\frac{(\mathbf{L} + \mathbf{D})}{\Delta t} - \frac{\mathbf{R}}{2} + \frac{\mathbf{\Omega}}{2} - \chi - \xi + 3\eta \right)$$

$$\mathbf{Z}_3 = \Delta z(\chi - \xi - 3\eta), \quad \mathbf{Z}_4 = \Delta z(\xi + \eta)$$

$$\chi = \sum_{i=1}^{M} \frac{\kappa_i}{p_i} \chi_i^1, \quad \xi = \sum_{i=1}^{M} \frac{\kappa_i}{p_i} \xi_i^1, \quad \eta = \sum_{i=1}^{M} \frac{\kappa_i}{p_i} \eta_i^1, \quad \Psi^n = \sum_{i=1}^{M} \frac{\kappa_i}{p_i} \Psi_i^n,$$

The general solutions of the MTL equations which are obtained in Eq. (30) and Eq. (31) are not valid for terminal voltages, which means that $\mathbf{V}_0^{n+1}$ and $\mathbf{V}_K^{n+1}$ need to be calculated. By adopting the technique used in [15], the terminal condition can be written as

$$\mathbf{V}_0^{n+1} = \mathbf{G}_2^{-1}\left(\mathbf{G}_3\mathbf{V}_0^n - \frac{2}{\Delta z}\mathbf{I}_{\frac{1}{2}}^{n+\frac{1}{2}} + \mathbf{G}_1\left(\mathbf{E}_{T,0}^{n+1} - \mathbf{E}_{T,0}^n\right)\right)$$

and

$$\mathbf{V}_K^{n+1} = \mathbf{Y}_1^{-1}\left(\mathbf{Y}_2\mathbf{V}_K^n + \frac{2}{\Delta z}\mathbf{I}_{K-\frac{1}{2}}^{n+\frac{1}{2}} + \mathbf{G}_1\left(\mathbf{E}_{T,K}^{n+1} - \mathbf{E}_{T,K}^n\right)\right)$$

where

$$\mathbf{G}_2 = \frac{\mathbf{C}}{\Delta t} + \frac{\mathbf{R}_0^{-1}}{\Delta z}$$

$$\mathbf{G}_3 = \frac{\mathbf{C}}{\Delta t} - \frac{\mathbf{R}_0^{-1}}{\Delta z}$$

$$\mathbf{Y}_1 = \frac{\mathbf{C}}{\Delta t} + \frac{\mathbf{R}_L^{-1}}{\Delta z}$$

$$\mathbf{Y}_2 = \frac{\mathbf{C}}{\Delta t} - \frac{\mathbf{R}_L^{-1}}{\Delta z}$$

$\mathbf{R}_0$ and $\mathbf{R}_L$ are the internal resistances which are connected to the sending end and receiving end of the line, respectively.

5. RESULTS AND DISCUSSION

In this part, the developed transmission line-plane wave coupling model is applied to show the effect of multilayer soil conductivities, elevation angle, polarization, and layer thicknesses on the induced voltages at the ends of the line. To do this, we consider a model composed of three conductors characterized by the same radius r and on height h_1 for the first conductor, h_2 for the second and h_3 for the third conductor, placed above a three-layer soil at positions $x_1 = 0\,\text{m}$, $x_2 = 2.5\,\text{m}$, $x_3 = 5\,\text{m}$ (Fig. 2(a)). The
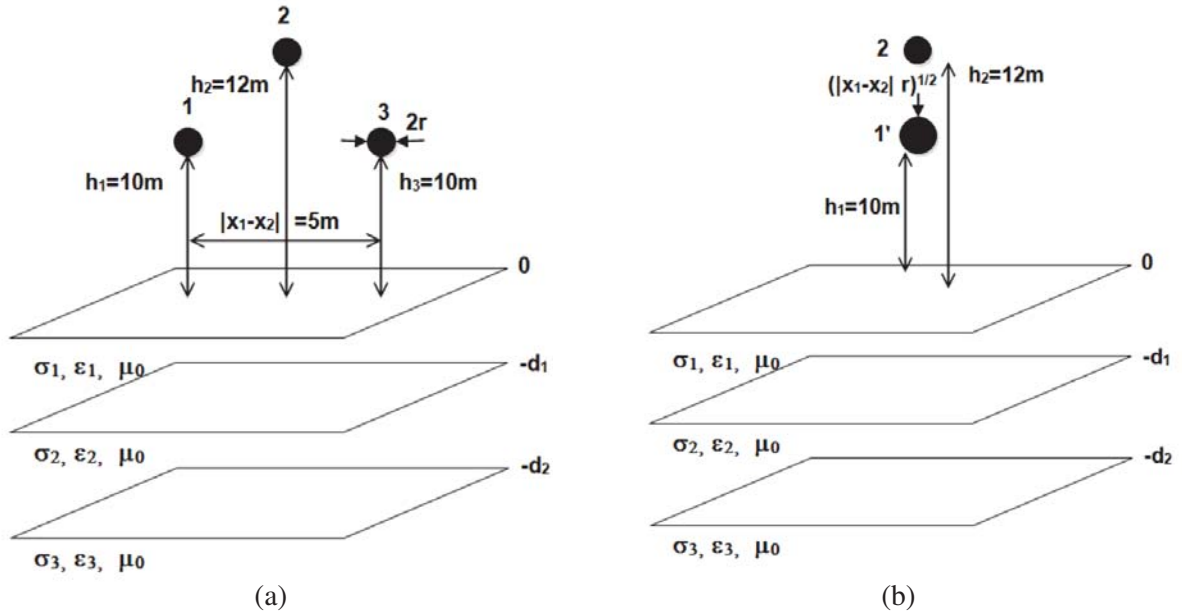

Figure 2. (a) Three-conductor transmission line configuration (TCM). (b) Equivalent two-conductor transmission line (ETCM).

upper layer is characterized by a conductivity σ_1 and permittivity ϵ_1 with a height d_1; the middle layer has the permittivity ϵ_2 and conductivity σ_2 with a thickness $d_2 - d_1$; the bottom layer is characterized by a permittivity ϵ_3 and conductivity σ_3; the three layers have the same permeability μ_0. For each layer, the electrical parameters are assumed to be constant. The internal resistances of the source and load are respectively set at $\mathbf{R}_0 = \mathrm{diag}(50, 50, 50)\Omega$ and $\mathbf{R}_L = \mathrm{diag}(100, 100, 100)\Omega$. diag stands for diagonal.

As indicated above, the determination of the induced voltages along the line relies primarily on the computation of the reflected field at the air-ground interface with precision. Fig. 3 illustrates the impact of different values of N used in expression (17) on the reflected field. The simulations here provided have the following assumptions: the plane wave is of vertical polarization of angles $\theta = 80°$, $\phi = 0°$, $\gamma = 0°$ and evaluated at the position ($x_1 = 0\,\mathrm{m}$, $h_1 = 10\,\mathrm{m}$, $l_z = 10\,\mathrm{m}$); the ground is formed of three layers of thicknesses $d_1 = 1\,\mathrm{m}$ and $d_2 - d_1 = 2\,\mathrm{m}$; the bottom layer is semi-infinite; the electrical parameters of the layers are $\sigma_1 = 10^{-4}\,\mathrm{S/m}$, $\sigma_2 = 10^{-3}\,\mathrm{S/m}$, $\sigma_3 = 10^{-2}\,\mathrm{S/m}$, $\varepsilon_{rg1} = \varepsilon_{rg3} = 10$, $\varepsilon_{rg2} = 12$. The accuracy of this approximation is for a value of $8 < N < 10$ as shown by comparison with FFT (Fig. 3). The value of N equal to 10 is adopted to accurately estimate the primary field for all the parameters involved.
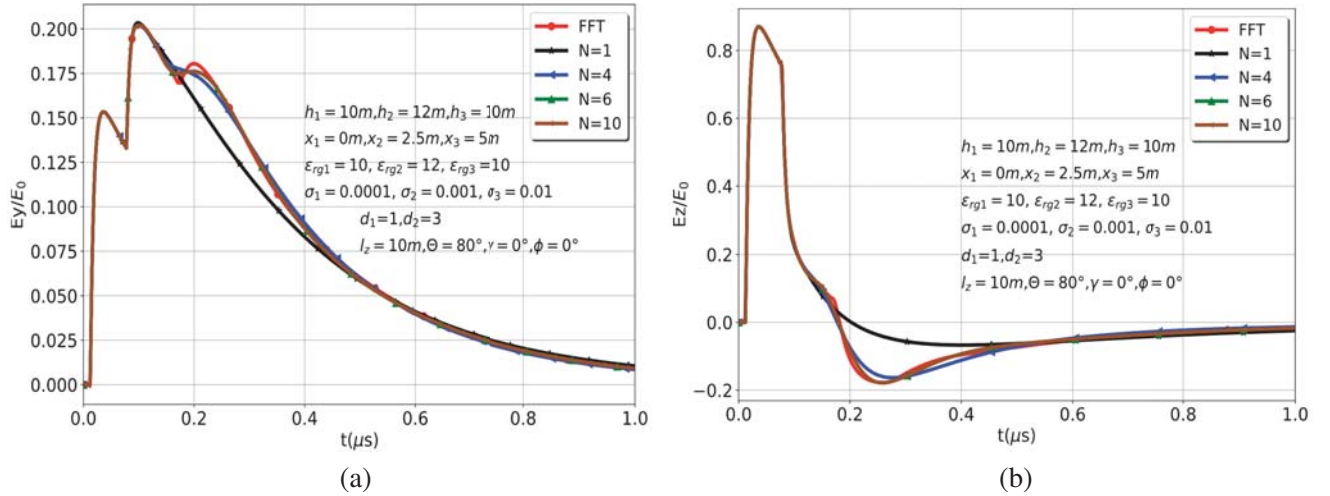

Figure 3. Reflected electric field for different values of N compared with the reference waveform obtained via FFT.

Figure 4(a) gives the response for different polarization angles ($\gamma = 0°$, $30°$, $60°$, $90°$), and the voltage response is lower for the case of horizontal polarization. Note that the voltage peak value decreases as the polarization angle increases. The voltage indicated in the figure is normalized with respect to V_0. The behavior of earth thickness d_1 of the first layer on the transient voltage for a vertical polarization is illustrated in Fig. 4(b). Due to the small conductivity ($\sigma_1 = 0.0001\,\mathrm{S/m}$) of the first layer, the losses in the soil become greater as d_1 increases, which is reflected in the decrease in voltage at the early time. The same observation can be made concerning the variation of the voltage at the near end of the line as a function of the thickness of the second layer for $d_1 = 0.5\,\mathrm{m}$. In addition, in the case of vertical polarization, the depth of the second layer has an effect on the pulse width.

To validate the proposed method, the two-conductor transmission line over a two-layer soil introduced in [20] is considered. The line configuration is shown in Fig. 5. The conductors are located at ($x_1 = 0\,\mathrm{m}$, $h_1 = 10\,\mathrm{m}$) and ($x_2 = 5\,\mathrm{m}$, $h_2 = 10\,\mathrm{m}$), and both have a radius of $r = 2.5\,\mathrm{mm}$ and length of $l_z = 20\,\mathrm{m}$. The upper and bottom layers are characterized, respectively, by the conductivities $\sigma_1 = 0.001\,\mathrm{S/m}$ and $\sigma_2 = 0.01\,\mathrm{S/m}$, and both have a relative permittivity of $\varepsilon_{rg1} = \varepsilon_{rg2} = 10$. The load matrices are assumed to be diagonal and are defined by ($R_{0,ii} = 100\Omega$, $R_{L,ii} = 50\Omega$, $i = 1, 2$). The parameters in Eq. (16) are given by: $\alpha = 4 \times 10^6\,\mathrm{s^{-1}}$, $\beta = 4.76 \times 10^8\,\mathrm{s^{-1}}$, and $E_0 = 52.5\,\mathrm{(kV/m)}$. As observed in Fig. 6, the current FDTD-based method (solid curves) matches very well with the FFT results (dashed curves) reported in [20] for the case of vertical and horizontal polarizations. Note that the slight difference between the FFT and FDTD results is because the earth return impedance models
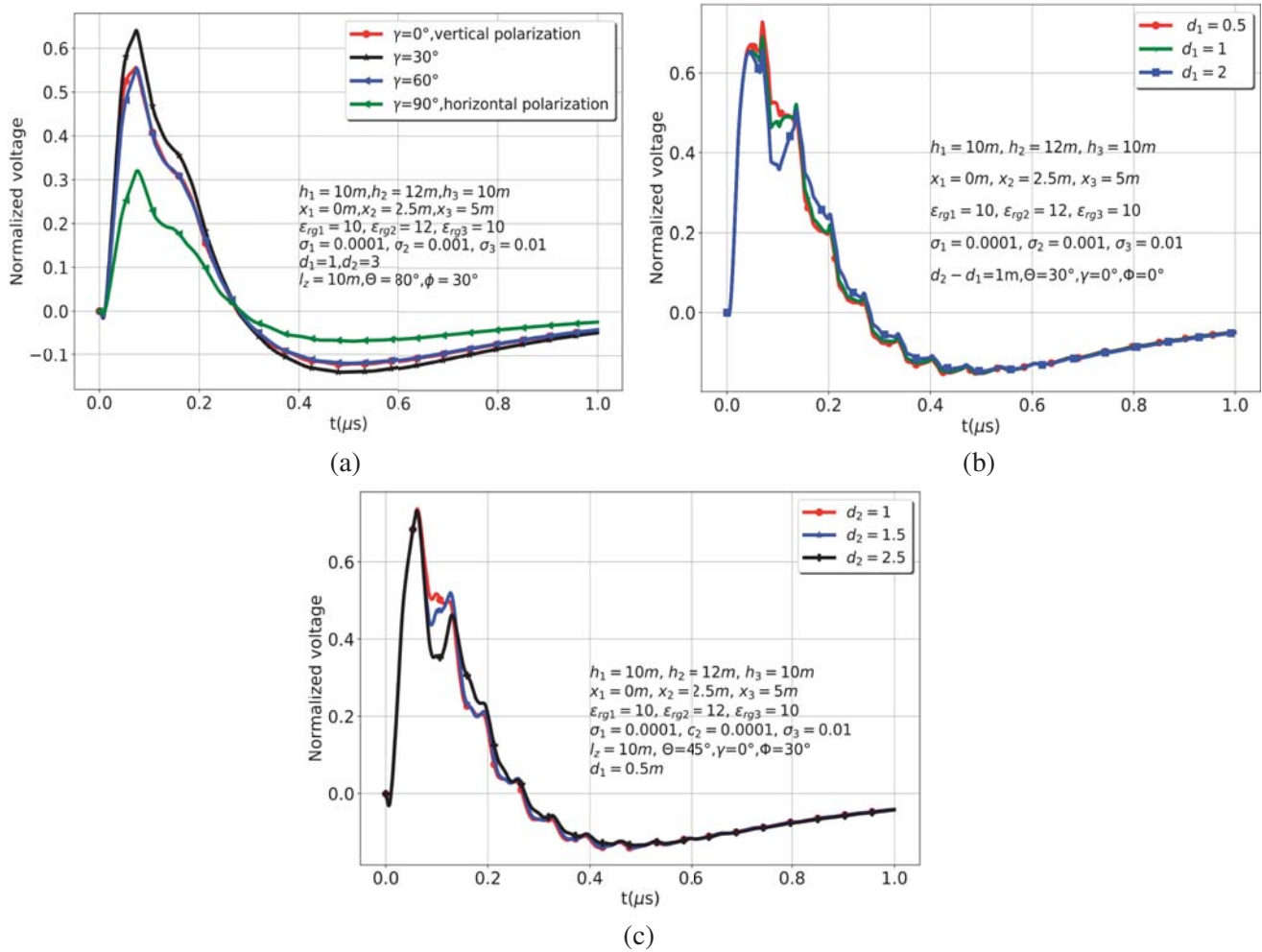
(a)

(b)

(c)

Figure 4. The transient response at the near end of the conductor 1 $(-V_1(0,t)/V_0)$ as a function of several parameters. (a) Polarization angles effect, (b) thickness d_1 effect, (c) thickness d_2 effect.
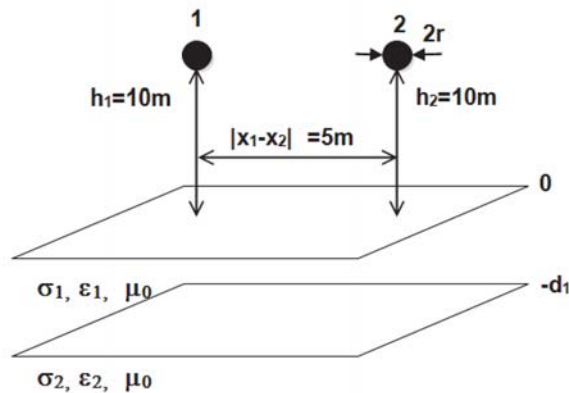

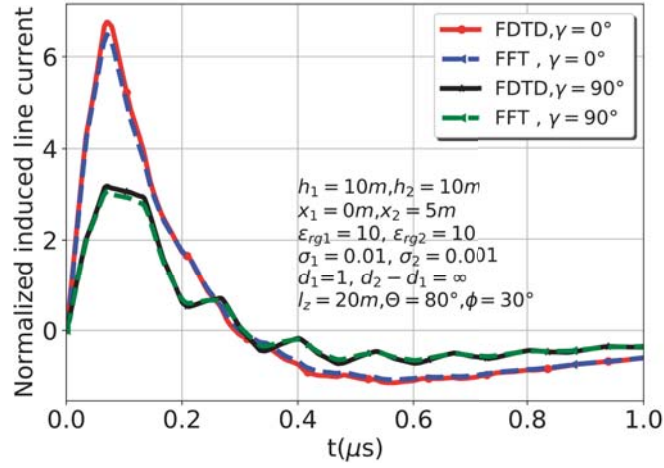**Figure 5.** Two-conductor overhead line configuration.

Figure 6. Comparison between the proposed model and the FFT presented in [20].
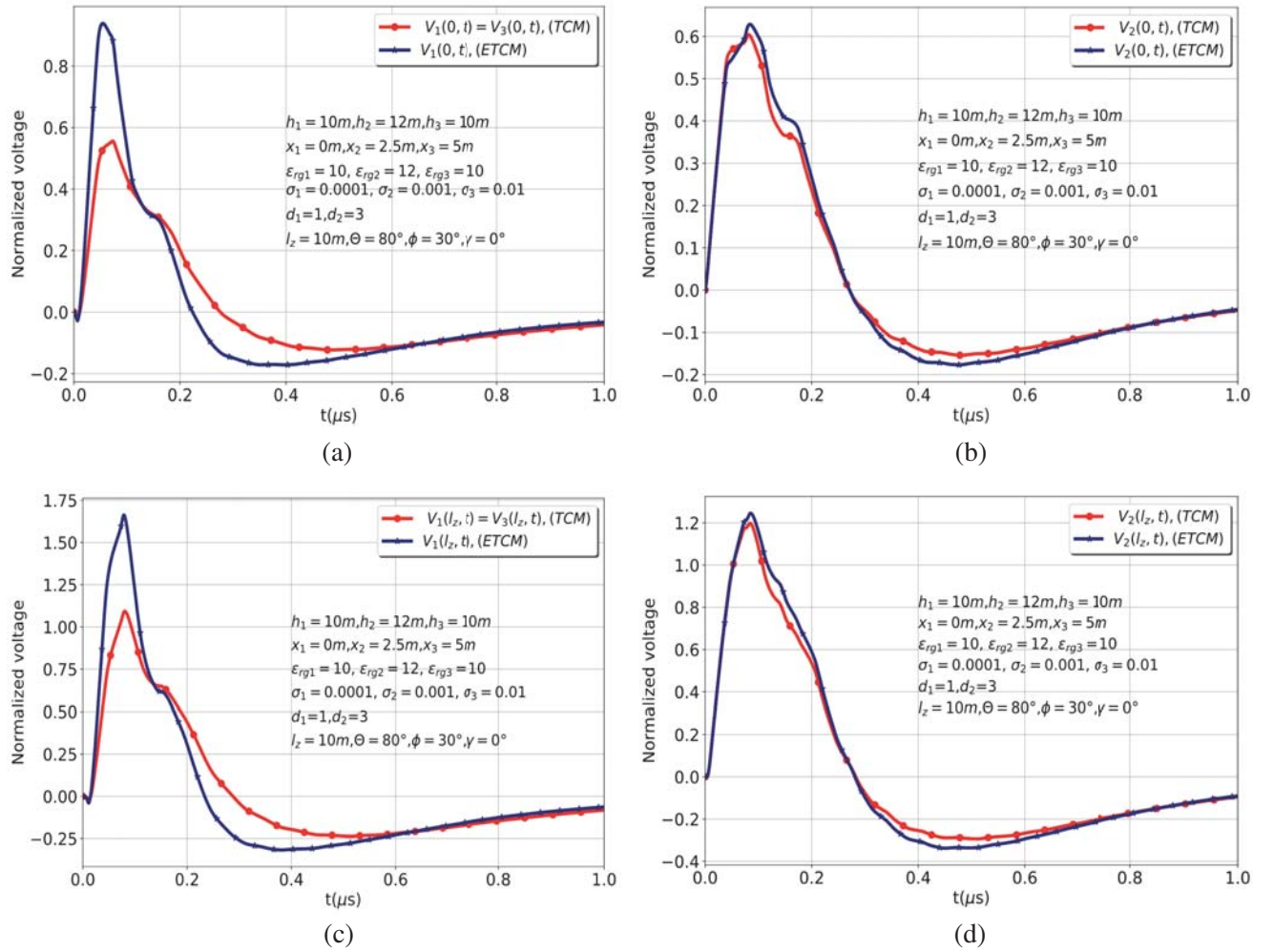

Figure 7. Induced voltages for TCM and ETCM at the near and far ends of the line, (a) $(-V_1(0,t)/V_0)$, (c) Conductors 1 and 3, (b) $(-V_2(0,t)/V_0)$, (d) Conductor 2.

used in this work and in [20] are not the same: this paper uses the Nakagawa model and [20] the Papadopoulos model [21]. In addition, the normalized induced current at the near end of the line shown in Fig. 6 is obtained by dividing the induced current by a constant current $I_0 = E_0 l_0 / \eta_0$. η_0 is the characteristic impedance of free space.

Figure 2(b) shows the equivalent model (ETCM) of the three conductors model (TCM), where we replace the two conductors placed at $h_{1,3} = 10$ m above the ground by an equivalent conductor $1'$ of the radius $r_{eq} = \sqrt{r|x_1 - x_3|}$, placed in the half distance of conductors 1 and 3.

The accuracy of reducing the TCM to ETCM by replacing the conductors $(1, 3)$ at the same height from the earth by conductor $1'$ is illustrated in Fig. 7. Despite the change of structure, the induced voltage in conductor 2 in the (TCM) can be reproduced in the same way using conductor $1'$ (ETCM), which means that instead of analyzing a system with three conductors model, it can be reduced to a two-conductor model.

For the elevation angle $\theta = 80°$, the induced voltages on conductors 1 and 3 are the same although the two conductors are at different positions ($x_1 = 0$ m and $x_3 = 5$ m). Indeed, this is due to the delay $t_a = \sqrt{\varepsilon_0 \mu_0} \cos(\theta) \sin(\phi)|x_1 - x_3|$ introduced by the plane wave which remains negligible both for $\theta = 80°$ (Figs. 7(a) and 8(a)) and for $\theta = 45°$ (Fig. 8(c)). Note that in Fig. 8(c) there is for the angle $\theta = 45°$ a very small difference between the voltage curves of conductors 1 and 3. From the results shown in Figs. 8(b) and 8(d), it appears that the estimation of the induced voltage on conductor 2 can
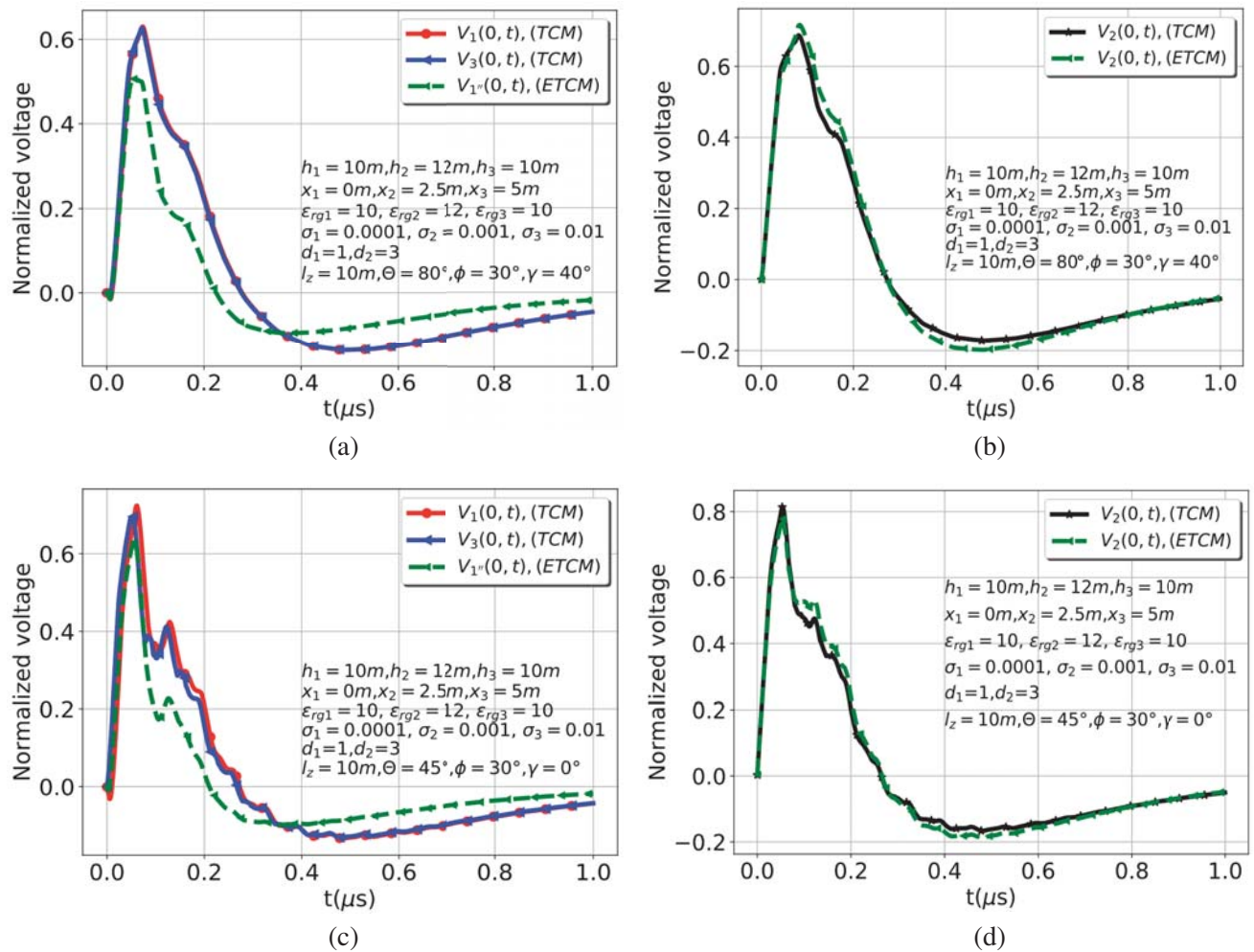

Figure 8. Induced voltages $(-V(0, t)/V_0)$ for TCM and ETCM at the near end (a) (c) of conductors 1, 3 and $1'$ for $\theta = (80°, 45°)$. (b), (d) Conductor 2 in TCM and ETCM for $\theta = (80°, 45°)$.

be obtained with accuracy by adopting the equivalent two-wire structure, whatever the elevation and polarization angles are. Furthermore, by dividing the induced voltage on the equivalent conductor by two, $v_{1''}(0, t) = v_{1, \, ETCM}(0, t)/2$, where $v_{1, \, ETCM}(0, t)$ is the voltage at the near end of the equivalent conductor, the equivalent model also provides an acceptable estimate of the peak induced voltage on conductors 1 and 3 as shown in Figs. 8(a) and 8(c).

6. CONCLUSION

In this paper, the transient voltage on an overhead line in the presence of stratified earth excited by a plane wave directly in the time domain has been determined. The advantage of the proposed method arises from the fact that the expressions of the earth return impedance and the Fresnel coefficients have been established directly in the time domain, by exploiting the (VF) and the Graver Stehfest algorithm. The results show that the transient voltage on the line is greater for the case of the vertical polarization than the horizontal polarization. In addition, the induced voltage increases for small thickness values of the first layer, and the increase in the duration of the transient waveform is due to the increase in the thickness of the second layer especially when the conductivities of the top layer and the second layer are small. Note that the method developed in this paper can be generalized to study the influence of soil stratification on lightning-induced voltages on an overhead line provided that the field created by a lightning channel in the presence of multi-layered soil is properly determined. Finally, the equivalent model composed of two conductors provides a good result since it is able to correctly estimate the induced voltage on the conductor placed between the other two.

REFERENCES

1. Tesche, F. M., M. Ianoz, and T. Karlsson, *EMC Analysis Methods and Computational Models*, J. Wiley and Sons, Inc., New York, 1997.
2. Doric, V., D. Poljak, and V. Roje, "Electromagnetic field coupling to multiple finite length transmission lines above an imperfect ground," *2003 IEEE International Symposium on Electromagnetic Compatibility, 2003, EMC '03*, Vol. 1, 595–598, Istanbul, Turkey, 2003.
3. Rachidi, F., "A review of field to transmission line coupling models with special emphasis to lightning induced voltages on overhead lines," *IEEE Transactions on Electromagnetic Compatibility*, Vol. 54, No. 4, August 2012.
4. Kordi, B., J. Lovetri, and G. E. Bridges, "Finite-difference analysis of dispersive transmission lines within a circuit simulator," *IEEE Transactions on Power Delivery*, Vol. 21, No. 1, January 2006.
5. Barnes, P. R. and F. M. Tesche, "On the direct calculation of a transient plane wave reflected from a finitely conducting half-space," *OAK Ridge National Laboratory (Theor. Note 358)*, December 5, 1990.
6. Antonijevic, S. and D. Poljak, "A novel time-domain reflection coefficient function: TM case," *IEEE Transactions on Electromagnetic Compatibility*, Vol. 55, No. 6, December 2013.
7. Stehfest, H., "Numerical inversion of Laplace transforms algorithm, Algorithm 368," *Commun. ACM*, Vol. 13, No. 1, 47–49, 1970.
8. Lu, T., L. Qi, and X. Cui, "Effect of multilayer soil on the switching transient in substations," *IEEE Transactions on Magnetics*, Vol. 42, No. 4, 843–846, April 2006.
9. Qi, L., X. Cui, and L. Li, "Transient plane wave coupling to overhead line above a multi-layer soil," *2006 IEEE International Symposium on Electromagnetic Compatibility, 2006, EMC 2006*, 669–673, Portland, OR, USA, 2006.
10. Agrawal, A. K., H. J. Price, and S. H. Gurbaxani, "Transient response of multiconductor transmission line excited by a nonuniform electromagnetic field," *IEEE Transactions on Electromagnetic Compatibility*, Vol. 22, 119–129, 1980.
11. Born, M., E. Wolf, A. Bhatia, P. Clemmow, D. Gabor, A. Stokes, and W. Wilcock, *Principles of Optics: Electromagnetic Theory of Propagation, Interference and Diffraction of Light*, 7th Edition, Cambridge University Press, Cambridge, 1999.

12. Nakagawa, N., A. Ametani, and K. Iwamoto, "Further studies on wave propagation in overhead lines with earth return: Impedance of stratified earth," *Proc. IEE*, Vol. 120, No. 12, 1521–1528, 1973,

13. Sunde, E. D., *Earth Conduction Effects in Transmission Systems*, 99–139, 2nd Edition, Dover Publications, 1968.

14. Gustavsen, B. and A. Semlyen, "Rational approximation of frequency-domain responses by vector fitting," *IEEE Trans. Power Del.*, Vol. 14, No. 3, 1052–1061, July 1999.

15. Paul, C. R., *Analysis of Multiconductor Transmission Lines*, Wiley, New York, 1994.

16. Yee, K., "Numerical Solution of initial boundary value problems involving Maxwell's equations in isotropic media," *IEEE Transactions on Antennas and propagation*, Vol. 14, 302–307, 1966.

17. Stratton, J. A., *Electromagnetic Theory*, McGraw-Hill, New York, 1941.

18. Lahmidi, A., A. Maaouni, and Z. Belganche, "Padé approximation for time-domain plane wave reflected from a lossy earth," *J. Phys. Commun.*, Vol. 2, 105001, 2018.

19. Lahmidi, A. and A. Maaouni, "Time-domain analysis of overhead line in presence of stratified earth," *Progress In Electromagnetics Reasearch M*, Vol. 88, 133–144, January 2020.

20. Belganche, Z., A. Maaouni, A. Mzerd, and A. Lahmidi, "Plane wave coupling to overhead lines over stratified earth," *2018 Progress In Electromagnetics Research Symposium (PIERS — Toyama)*, 2212–2219, Toyama, August 1-4, 2018.

21. Papadopoulos, T. A., G. K. Papagiannis, and D. P. Labridis, "A generalized model for the calculation of the impedances and admittances of overhead power lines above stratified earth," *Electric Powers systems Research*, Vol. 80, 1160–1170, 2010.